



Intraplate volcanism in the Danube Basin of NW Hungary: 3D geophysical modelling of the Late Miocene Pásztori volcano

Jaroslava Pánisová¹ · Attila Balázs² · Zsófia Zalai³ · Miroslav Bielik^{1,4} · Ferenc Horváth⁵ · Szabolcs Harangi^{6,7} · Sabine Schmidt⁸ · Hans-Jürgen Götze⁸

Received: 1 August 2017 / Accepted: 24 November 2017 / Published online: 6 December 2017
© Springer-Verlag GmbH Germany, part of Springer Nature 2017

Abstract

Three-dimensional geophysical modelling of the early Late Miocene Pásztori volcano (ca. 11–10 Ma) and adjacent area in the Little Hungarian Plain Volcanic Field of the Danube Basin was carried out to get an insight into the most prominent intracrustal structures here. We have used gridded gravity and magnetic data, interpreted seismic reflection sections and borehole data combined with re-evaluated geological constraints. Based on petrological analysis of core samples from available six exploration boreholes, the volcanic rocks consist of a series of alkaline trachytic and trachyandesitic volcanoclastic and effusive rocks. The measured magnetic susceptibilities of these samples are generally very low suggesting a deeper magnetic source. The age of the modelled Pásztori volcano, buried beneath a 2 km-thick Late Miocene-to-Quaternary sedimentary sequence, is 10.4 ± 0.3 Ma belonging to the dominantly normal C5 chron. Our model includes crustal domains with different effective induced magnetizations and densities: uppermost 0.3–1.8 km thick layer of volcanoclastics underlain by a trachytic-trachyandesitic coherent and volcanoclastic rock units of a maximum 2 km thickness, with a top situated at minimal depth of 2.3 km, and a deeper magmatic pluton in a depth range of 5–15 km. The 3D model of the Danube Basin is consistent with observed high ΔZ magnetic anomalies above the volcano, while the observed Bouguer gravity anomalies correlate better with the crystalline basement depth. Our analysis contributes to deeper understanding of the crustal architecture and the evolution of the basin accompanied by alkaline intraplate volcanism.

Keywords Multiphase intraplate volcanism · 3D modelling · Potential fields · Seismic interpretation · Danube Basin

✉ Jaroslava Pánisová
geofjapa@savba.sk

¹ Division of Geophysics, Earth Science Institute of the Slovak Academy of Sciences, Dúbravská cesta 9, 840 05 Bratislava, Slovakia

² Faculty of Geosciences, Utrecht University, Budapestlaan 6, 3508 TA Utrecht, The Netherlands

³ Department of Geophysics and Space Science, Eötvös Loránd University, Pázmány Péter st. 1/C, 1117 Budapest, Hungary

⁴ Department of Applied and Environmental Geophysics, Faculty of Natural Sciences, Comenius University, Mlynská dolina, Ilkovičova 6, 842 15 Bratislava, Slovakia

⁵ Geomega Ltd, Budapest, Hungary

⁶ Department of Petrology and Geochemistry, Eötvös Loránd University, Pázmány Péter st. 1/C, 1117 Budapest, Hungary

⁷ MTA-ELTE Volcanology Research Group, Budapest, Hungary

⁸ Institute of Geosciences, Christian-Albrechts-University, Otto-Hahn-Platz 1, 24118 Kiel, Germany

Introduction

The Carpathian–Pannonian region of Central Europe contains various Miocene–Pliocene volcanic fields; their formation is primarily controlled by the closure of two oceanic realms and subsequent Miocene syn-rift extension and post-rift basin evolution (Konecný et al. 2002; Harangi and Lenkey 2007; Horváth et al. 2015). Localization of extension and associated volcanism are often determined by lithospheric rheological heterogeneities, such as zones related to former subduction and collision phases or large-scale fault or detachment zones (Rollet et al. 2002; Balázs et al. 2017). Similar to other Miocene extensional back-arc basins in the Mediterranean, such as the Tyrrhenian or the Alboran Sea (e.g., Faccenna et al. 2014), evolution of the Pannonian Basin was associated with the extensional reactivation of former thrusts and nappe contacts. Extension was followed by continuous post-rift subsidence and alkaline volcanism (e.g., Tari 1996; Horváth et al. 2015).

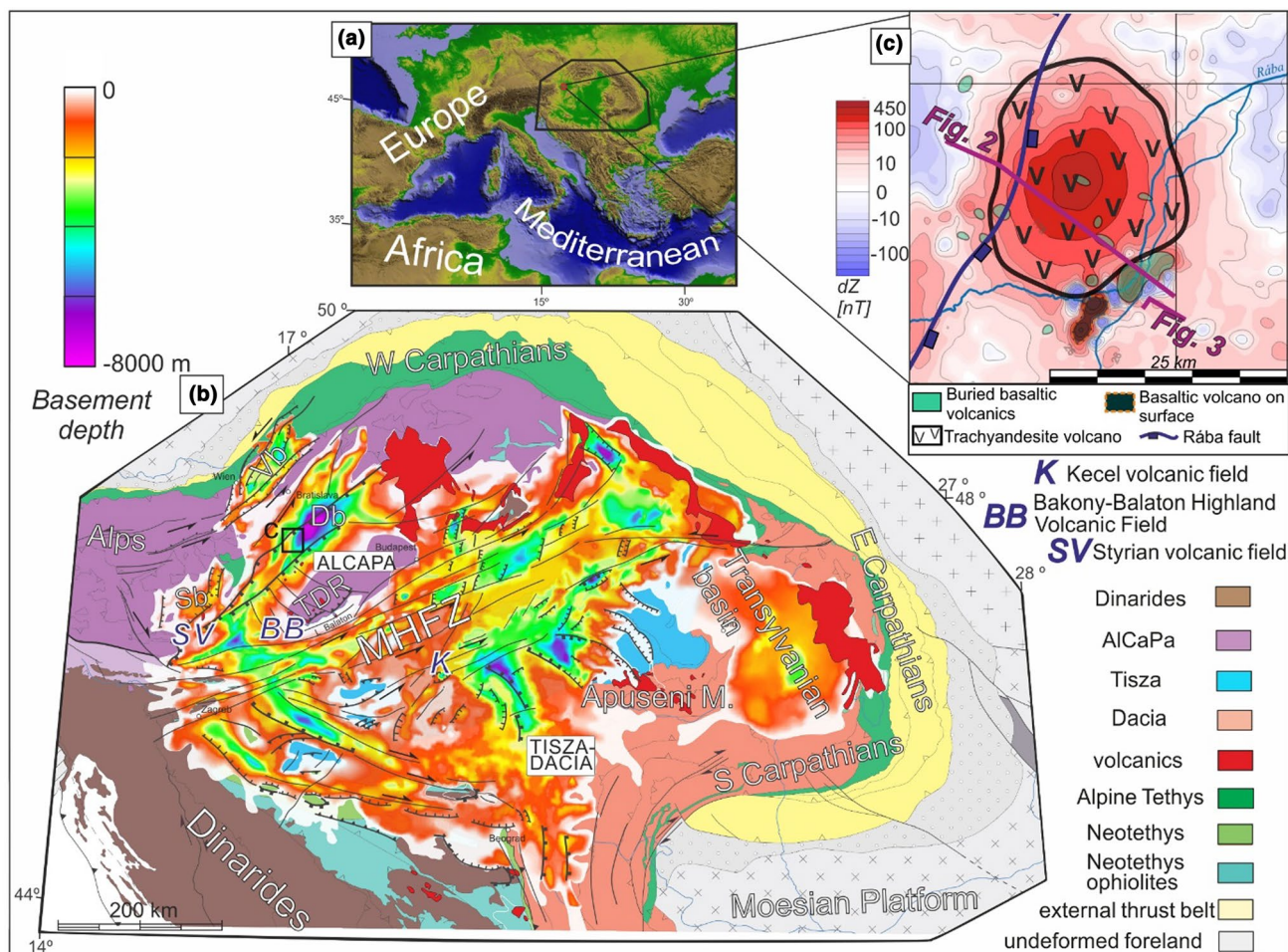


Fig. 1 **a** Topography and location of the Pannonian Basin system of the Mediterranean region, **b** simplified tectonic map of the Alps—Carpathians Dinarides region (modified after Schmid et al. 2008) overlain by the Miocene–Quaternary sedimentary thickness (in meters) of the Vienna (Vb), Pannonian and Transylvanian basins.

One of the most extended sub-basins of the region is the Danube Basin characterized by fairly high crustal and lithospheric thinning factors (locally could exceed 2; Lenkey et al. 2002). It is located in NW Hungary and SW Slovakia (Fig. 1). The Little Hungarian Plain (LHP) represents the southern part of the SW–NE elongated Danube Basin. It hosts the Mio-Pliocene alkaline basaltic Little Hungarian Plain Volcanic Field (LHPVF), located between the Transdanubian Central Range (TDR) and the foothills of the Eastern Alps (Harangi et al. 1995a; Harangi 2001). A noteworthy feature of this field is the subsurface Miocene volcanic complex of the Pásztori volcano. It is a suitable place to study the volcanic evolution of such an extensional basin due to the dense seismic and borehole coverage and available gravity and magnetic anomaly maps.

Unlike most of the intra-Carpathian volcanoes associated with subduction of the Pásztori volcano and adjacent area

MHFZ Mid-Hungarian Fault Zone, *Db* Danube Basin, *TDR* Transdanubian Range, *Sb* Styrian Basin (modified after Balázs et al. 2017), **c** magnetic ΔZ anomaly map (after Kiss and Gulyás 2006b) of the Danube Basin overlain by the location of surface and subsurface igneous bodies

are interpreted to be a typical example of multiphase intra-plate volcanism. The Late Miocene trachyandesite–trachyte volcanism produced thick (more than 1000 m) stratovolcanic complex at the central axis of LHP (Harangi et al. 1995a; Harangi 2001), which was followed by basaltic volcanism after 5–6 Ma of volcanic quiescence (Balogh et al. 1986; Wijbrans et al. 2007). The Pásztori volcano is currently buried beneath a 2 km-thick Late Miocene-to-Quaternary sedimentary sequence.

Seismic and well data interpretation coupled with an integrated potential field modelling can provide valuable information from larger depths too, where other geophysical methods are hardly applicable (e.g., Götze et al. 2007; Reynisson et al. 2009; Alvers et al. 2014; Tschirhart and Pehrsson 2016). Magmatic intrusions beneath volcanic structures have been studied worldwide using combination of several geophysical methods to get valuable constraints on

their subsurface structural configuration. Gudmundsson and Milsom (1997) studied the structure of subglacial Grímsvötn volcano in Iceland using gravity and magnetic data to map the distribution and size of magma bodies, caldera fill, and subvolcanic intrusions, and to investigate the link between the models obtained from two-and-a-half forward modelling and the sources of the high geothermal heat flux. Wamalwa et al. (2013) focused on the Menengai volcanic system of the East African Rift in Kenya with a detailed quantitative analysis of gravity and broadband magnetotelluric data to investigate its geothermal potential. Blaikie et al. (2014) published a complex 3D models of multi-vent maar diatreme systems of four maars from the Newer Volcanics Province of SE Australia obtained by means of 3D potential field modelling to get an improved understanding of their eruptive histories.

One of the first geophysical models of the Pásztori volcano calculated using gravity forward modelling was published by Nemesi et al. (1994). The authors approximated the volcano by simple rectangular 2D prism of constant susceptibility of 0.088 SI. The prism had 14 km in length with top situated at 6 km depth. Mattick et al. (1996) investigated the hydrocarbon potential of the LHP by means of interpreted seismic reflection and wells data. Kronome et al. (2014) adopted the interpretation of Mattick et al. (1996) that this buried volcano is situated on the hanging wall of a SE-dipping first-order normal fault. In their 2D geological section, the volcanic products are intercalated with the sedimentary fill of the subsiding basin. The poor signal-to-noise ratio at larger depths prevented reliable interpretation of the volcanic edifice at a crustal scale.

In this study, we present high-resolution geophysical data and attempt to shed new light on the intra-crustal structures beneath the sedimentary basins of the LHP compiling an integrated 3D gravity and magnetic model which is based on interpreted seismic reflection sections and well data analysis. The new, three-dimensional model of the buried volcanic structures is built by a combination of conventional polyhedral geometries with voxels in the IGMAS+ software (Schmidt et al. 2011). Petrological analysis helps to understand the multiphase evolution of the investigated volcanic complex.

Geological setting

The Pannonian Basin of Central Europe is traditionally considered as a continental back-arc basin, where the roughly East–West oriented ~220–290 km of Miocene extension is accommodated by the roll-back of the Carpathians and/or Dinaric slabs (Fig. 1, e.g., Matenco and Radivojević 2012; Horváth et al. 2015). Similar to other Mediterranean back-arc basins, extensional basin

formation followed a pre-Neogene orogenic evolution that resulted from the opening and subsequent closure of two oceanic realms, the Triassic–Cretaceous Neotethys and Middle Jurassic–Paleogene Alpine Tethys (e.g., Schmid et al. 2008 and references therein). Former subduction process can be inferred from the presence of obducted ophiolites, flysch in the accretionary wedge in the Carpathians and Miocene calc-alkaline volcanism (Fig. 1b). The presence of upper crustal heterogeneities, in terms of pre-existing shear zones and nappe systems, had a first-order control on the style of deformation and syn-rift basin evolution (e.g., Tari et al. 1999). The general extensional geometry of the basin is characterized by individual sub-basins filled by ~1–3.5 km of lower to lowermost Late Miocene syn-kinematic deposits, furthermore overlain by a 1.5–3.5 km-thick post-extensional sedimentary cover (Balázs et al. 2016). Extensional basin formation as well as the subsequent post-rift thermal evolution was accompanied by intense volcanism (Konecný et al. 2002; Harangi et al. 1995a, 2015; Harangi and Lenkey 2007).

The deepest and largest sub-basin of the Pannonian region is the Danube Basin (cf., Sztanó et al. 2016) at the foothills of the Eastern Alps, containing a Miocene-to-Quaternary sedimentary thickness of up to ~8 km (Fig. 1b). Its pre-Neogene basement is composed by various low-grade metamorphic rocks of Paleozoic age and they are structurally assigned to the Upper Austroalpine nappe system (Tari et al. 1999). The low-angle Rába fault zone (Fig. 1b, c) is traditionally considered to separate the Austroalpine nappes from the structurally overlying Transdanubian Range unit (Szafián et al. 1999). The latter is built up by low-grade metamorphic and non-metamorphosed Permian–Cretaceous sedimentary cover including predominantly Triassic carbonates (Szafián et al. 1999; Haas et al. 2010; Horváth et al. 2015). The “Rába line” played the role of a complex Miocene dominantly low-angle normal and to a lesser extent strike-slip fault zone which strongly reworked the primary Cretaceous nappe contact of the Austroalpine and the Transdanubian Range units (Tari 1996). Late Miocene-to-Quaternary evolution of the Danube Basin is associated with thermal subsidence and the deposition of several kilometres thick siliciclastic sediments with intercalated tuff layers that are related to the 11–10 Ma activity of the Pásztori volcano (Harangi et al. 1995a). Furthermore, alkaline basaltic magmatism took place ca. 5.5–4 Ma (Balogh et al. 1986; Wijbrans et al. 2007; Harangi et al. 2015) in the basin. The final cessation of extension was followed by large-scale inversion in the Pannonian Basin from ~8–7 Ma manifested in contractional structures near the Dinaric margin, dominantly transcurrent kinematics elsewhere and accelerated differential vertical movements (Bada et al. 2007).

Input data and constraints

Volcanology and petrology of the Pásztori volcano

The Pásztori volcano was drilled by several exploration wells during the 1960–1980s (Kőrössi 1987). It has an approximately 20–25 km diameter and one of the boreholes (Pá-1) penetrated more than 1500 m of volcanic formations. None of the three boreholes [Pá-1: (517,986, 244,415 m); Pá-2: (515,217, 243,086 m); and Pá-4: (516,718, 248,799 m) EOV coordinates] in the central part of the volcano reached the pre-Cenozoic basement of the volcanic edifice. Based on the occasional drilling cores, the lower (min. 800 m thick) segment of the volcanic edifice is built up by alkaline trachyte lavas and intercalated pyroclastic and volcanoclastic beds (Schléder 2001). This section is overlain by trachyandesitic lava flows and volcanoclastic breccias, interpreted partly as redeposited mass flow deposits. Alkaline basaltic rocks occur subordinately in the upper part of the volcanic succession that could represent either dykes or minor lava flows. They have remarkable trace element compositional similarities with the 10–11 Ma basalts found in Burgenland suggesting possible genetic relationships (East Austria; Harangi et al. 1995a; Harangi 2001). The volcanoclastic layers are often intercalated with deep water siliciclastic muds and shales. Noteworthy, mixing of trachytic magma and water-saturated fine-grained sediment resulted in peperitic formations with a fluidal textural form. This reflects fluid–fluid mingling of magma and fluidized or liquefied sediment (Martin and Németh 2007), possibly at the base of the lava flow (Németh et al. 2008; McLean et al. 2016). Based on the volcanological features, subaerially exposed paleovolcano is interpreted that formed an island in the shallow shelf margin environment of Lake Pannon.

The alkaline trachytes have a porphyritic texture with alkaline feldspar phenocrysts, which show dissolution to pure Na- and K-rich feldspar endmembers. Quartz, aegirine, occasional riebeckite in addition to alkali feldspars constitute the groundmass mineral phases. The trachyandesites consist of both plagioclase and sanidine with a wide compositional spectrum and contain clinopyroxene (ferroan diopside to aegirine-augite) as well as kaersutite and biotite. The basalts are olivine- and clinopyroxene-phyric rocks. Trace element and isotope compositions of the volcanic rocks suggest that dominantly closed system fractional crystallization from a parental alkaline basaltic magma could lead to the trachyandesitic and trachytic evolved magmas (Harangi et al. 1995a; Harangi 2001).

Constraints from boreholes

Induced magnetic susceptibility was measured on 68 samples from six different boreholes (Pá-1, Pá-2, Pá-4, Tét-4, Tét-5, Tét-6) that penetrated the volcanic complex. Our measurements were carried out with a Bartington MS2 instrument, which has a nominal error of $\pm 5\%$. Every sample was measured on three distinct sides; these three measurements were then averaged to give the susceptibility of the sample. These susceptibilities are in Table 1 averaged by rock type and wells. Note that the susceptibilities span four orders of magnitude, trachytes, and lapilli tuffs having the lowest susceptibility values. As expected, basalts and trachyandesite with biotite have the highest values due to their build-up minerals' paramagnetic properties and iron content.

We were able to obtain densities from three samples, a trachyte from 2857 to 2860 m in Tét-4, one from 3392 to 3392.5 m in Pá-1, and a trachyandesite with biotite from 2681–2683 m in Pá-1. The densities were measured with the water immersion method. The densities (ρ) can be obtained from the measured weight of the sample in air (m_a) and the weight immersed in water (m_w) using the following equation:

$$\rho = \frac{m_a}{m_a - m_w}.$$

The nominal error of the measured densities is $\pm 2\%$.

The measured magnetic susceptibilities of these samples are generally very low, about 0.00005–0.0005 SI (see Table 1; Clark and Emerson 1991; Hunt and Moskowitz 1995).

2D seismic reflection data

Our analysis of the Pásztori volcano and adjacent structures contains the interpretation of a network of 27 seismic profiles from the Danube Basin calibrated by well data. The amplitude, frequency, continuity, terminations, and the overall distribution of seismic reflectors and the patterns of the Bouguer gravity and magnetic anomaly maps (Kiss and Gulyás 2006a, b) supported the interpretation of the Miocene sediments and (sub)volcanic bodies. Subsequently, the mapped seismic horizons were converted from two-way travel time (TWT) to depth using standard VSP (vertical seismic profile) logs. The resulted depth maps were used to constrain the initial input geometries for the 3D gravity and magnetic modelling performed by the IGMAS+ software (Alvers et al. 2014; Schmidt et al. 2015).

Table 1 Measured average-induced magnetic susceptibility and density by rock type

Well number	MD (m)	Rock type	Average susceptibility (10^{-5} SI)	Standard deviation	Density (g cm^{-3}) ^a
Tét-4	3455–3457	Basalt (3)	35.66667	4.486896	
Tét-4	2857–2860	Trachyte (1)	6	0	2.504
Tét-5	2321–2324	Fluidal lapilli tuff (4)	189.8325	362.8031	
Tét-5	2864–2865	Trachyte (1)	18.67	0	
Tét-6	3073–3075	Trachyandesite (1)	11	0	
Tét-6	3074–3075	Lapilli tuff (5)	4.266	3.329899	
Tét-6	2857–2860	Fluidal trachyandesite (2)	3.665	3.768879	
Pá-1	1774–2517	Lapilli tuff (7)	16.80857	5.634668	
Pá-1	3392–3500	Trachyte (3)	6.11	1.837471	2.455
Pá-1	1985.5–1988.5	Red trachyandesite (1)	21.00	0	
Pá-1	2909–3238	Basalt (2)	7.835	0.233345	
Pá-1	2681–2683	Trachyandesite w/biotite (2)	466.335	631.213	2.77
Pá-2	2726.5–2727.5	Polimict coarse lapilli tuff (3)	9.666667	4.50925	
Pá-2	2183–2658	Trachyte (10)	6.799	3.019534	
Pá-2	1819–1823	Lapilli tuff (3)	15.11	7.648869	
Pá-2	2259–2060	Basalt (1)	122.67	0	
Pá-4	2005–2727	Lapilli (7)	13.76286	8.650624	
Pá-4	2083–2155	Basalt (2)	1864.33	1129.957	

Number in parenthesis indicate the number of samples

^a1 g cm^{-3} = 1000 kg m^{-3}

Magnetic and gravity data

The magnetic database in Hungary handled by the Hungarian Geological and Geophysical Institute (former ELGI) integrates several nationwide measurement campaigns, with the oldest dated back to the 1950s. The regional ground survey magnetic ΔZ database (more than 74,000 points, $0.79 \text{ point km}^{-2}$) complemented by a local surveys data in some part of the country was reprocessed and contoured into a ΔZ Anomaly Map of Hungary (Kiss and Gulyás 2006b). The map displays the vertical (ΔZ) component of the total magnetic field. The following parameters of the Earth's magnetic field in the region were utilized in the model: (1) an average inclination of 63.5° , (2) a declination = -1° , and (3) an average value of $46,700 \text{ nT}$ of the magnetic total field.

In this case study, the regional gravity data of Hungary are also used (Kiss and Gulyás 2006a). This gravity database consists of more than 380,000 randomly distributed gravity points, with survey density of 4 point km^{-2} on average. The gravity data were processed in a standard manner. The data were interpolated into grid producing the countrywide gravity map in a scale of 1:500,000 with a grid spacing of 500 m (Kiss and Gulyás 2006a). The Hungarian Bouguer anomaly map was constructed using a terrain correction density of 2.0 g cm^{-3} (Kiss 2006).

3D modelling with IGMAS+

To compile the three-dimensional model of the buried Pásztori volcano in the Danube Basin we get use of the IGMAS+ (Interactive Geophysical Modelling Assistant) program. It is a 3D geo-modelling software which is based on simultaneous forward modelling of gravity, gravity gradients, and magnetic fields (Schmidt et al. 2011, 2015; Götze 2014). The software platform IGMAS+ offers an interdisciplinary modelling approach integrating independent data sets from seismic, boreholes, and geology, and thus reducing the ambiguity of potential field inversion. The superposition of a voxel model and triangulated surfaces gives possibility to produce complex (“hybrid”) models allowing to describe geological structures in a more realistic way (Schmidt et al. 2011; Alvers et al. 2014).

First reference model

To reduce the inherent ambiguity in the interpretation of potential fields, we have integrated all available auxiliary geophysical data and geological information. This inherent nature of potential field causes that the same data can be explained by literally infinite number of mathematical models (Götze 2014). Of course, only a few of them are geologically feasible. The starting background model should

consist of all a-priori known triangulated horizontal interfaces extended far enough to avoid edge effects. In our case, the starting model geometry was constrained using following geological interfaces based on latest re-evaluated data sets: (1) pre-Cenozoic basement from Maros and Maigut (2011) and (2) Moho depths from Horváth et al. (2015). Real topography was not included into the model as the Bouguer gravity data are corrected for terrain effects and the elevation changes in studied area are negligible.

The boundary between upper and lower crust was defined as an average between the basement and the Moho. This interface attains 16.5 km in average in the studied territory of the LHP. Such approximation is in agreement with the previous studies by Kiss (2009) and Hetényi et al. (2015). Compaction of the sediments with depth is applied by a trend function $\rho(z) = 2.7 - 0.74 e^{-0.00087z}$ published by Mészáros and Zilahi-Sebes (2001). This density-depth function was based on re-evaluated well logs from boreholes located in the Transdanubia region that are deeper than 1000 m.

In the lowermost parts of the Pannonian basin, e.g., at depths of 5–8 km, the density of the sediments can locally attain 2.65 g cm^{-3} (e.g., Bielik 1998). As the exponential trend function gives higher values in the deepest parts of modelled sub-basins, we decided to split the sediments into two bodies on this threshold, the upper one with a compaction applied and the lower one with a defined constant density of 2.65 g cm^{-3} .

3D modelling procedure

The extended starting model was first divided into 47 NW–SE-directed vertical sections perpendicular to the strike of the structures in the sub-basin. The investigated area, clipped to the station bounds and containing the modelled volcanic bodies, consists of 30 sections. These vertical cross sections are carriers for the vertices of 2D polygons which are connected using automated triangulation procedure with the aim to produce the 3D model geometry (Schmidt et al. 2015). The gravitational and magnetic effects of homogeneous 3D polyhedrons are calculated using algorithm kernel based on analytical solution derived in Götze and Lahmeyer (1988), where two Gauss theorems are applied to transform the original volume integral into a line integral easily solvable using transformation of coordinates to local coordinate system of a triangle element (Götze 2014).

The interpreted seismic horizons (see exemplary reflection seismic transect in Fig. 2) were imported to the IGMAS+ as point sets and projected to particular sections, to roughly define the preliminary shape of the volcanic structures, mainly the tops of volcanic layers. Then, the geometries and physical properties (density and magnetic susceptibility) of the individual bodies were altered manually to get a sufficient match of the observed (measured) and

calculated magnetic curves in amplitude and shape. For the modelling of the magnetic field, only induced magnetization was taken into account. Based on new geochronologic data, the age of the Pásztori volcano is $10.4 \pm 0.3 \text{ Ma}$ belonging to the C5 chron, which is dominantly normal. Therefore, we have decided to neglect the remanent magnetization.

The modelling provided the interesting observation that the volcanic body generates only hardly recognizable signature in the gravity field. We had to split the upper crust into several geological units with different densities based on the pre-Cenozoic basement map of Haas et al. (2010) to fit the gravity fields. We were looking for the simplest configuration of the upper crustal units that will reproduce the Bouguer gravity anomaly map. The most important Rába and Répce faults divided the background density model of the upper crust into 33 several bedrock units of different densities. These crustal units numbered after Haas et al. (2010) are summarized in Table 2 by rock type and density range. The crystalline pre-Cenozoic basement in the surveyed area comprises of Paleozoic-to-Mesozoic metamorphic rocks (gneiss, mica schist, phyllite, limestone, dolomite, sandstone, etc.). The used densities shown in Table 2 are in agreement with values published in Eliáš and Uhmman (1968) and Szabó and Páncsics (1999).

Results

Seismic interpretation

Regional seismic profile (Fig. 2) over the research area of the Danube Basin shows 1.5–2.0 km of Late Miocene-to-Quaternary siliciclastic sediments underlain by the volcanic series of the Pásztori volcano and Middle Miocene syn-rift sediments. Late Miocene sedimentary succession of Lake Pannon onlaps and interfingers with the Pásztori volcanoclastics. Younger, basalt bodies within these Pannonian (s.l.) sediments are inferred (cf., Tari et al. 1999) by the high-amplitude magnetic anomalies (Fig. 1c) and their characteristic high-amplitude, discontinuous seismic facies (Fig. 3). The sharp seismic impedance contrast of such basalt bodies commonly results in blanketing the reflectors of the underlying sediments. Small-offset normal faults are present above the Pásztori volcano most probably related to minor magmatic activity and compaction effects. Seismic facies of the Middle Miocene sedimentary succession are characterized by gently divergent reflectors due to coeval normal fault offsets, their thickness increases towards the low-angle SE-dipping Rába fault zone (Fig. 2). Volcanoclastics show a variation of high and low-amplitude, continuous, divergent to (sub)-parallel seismic facies. Interpretation of the Pásztori volcanic body is mainly based on well data and the specific seismic facies

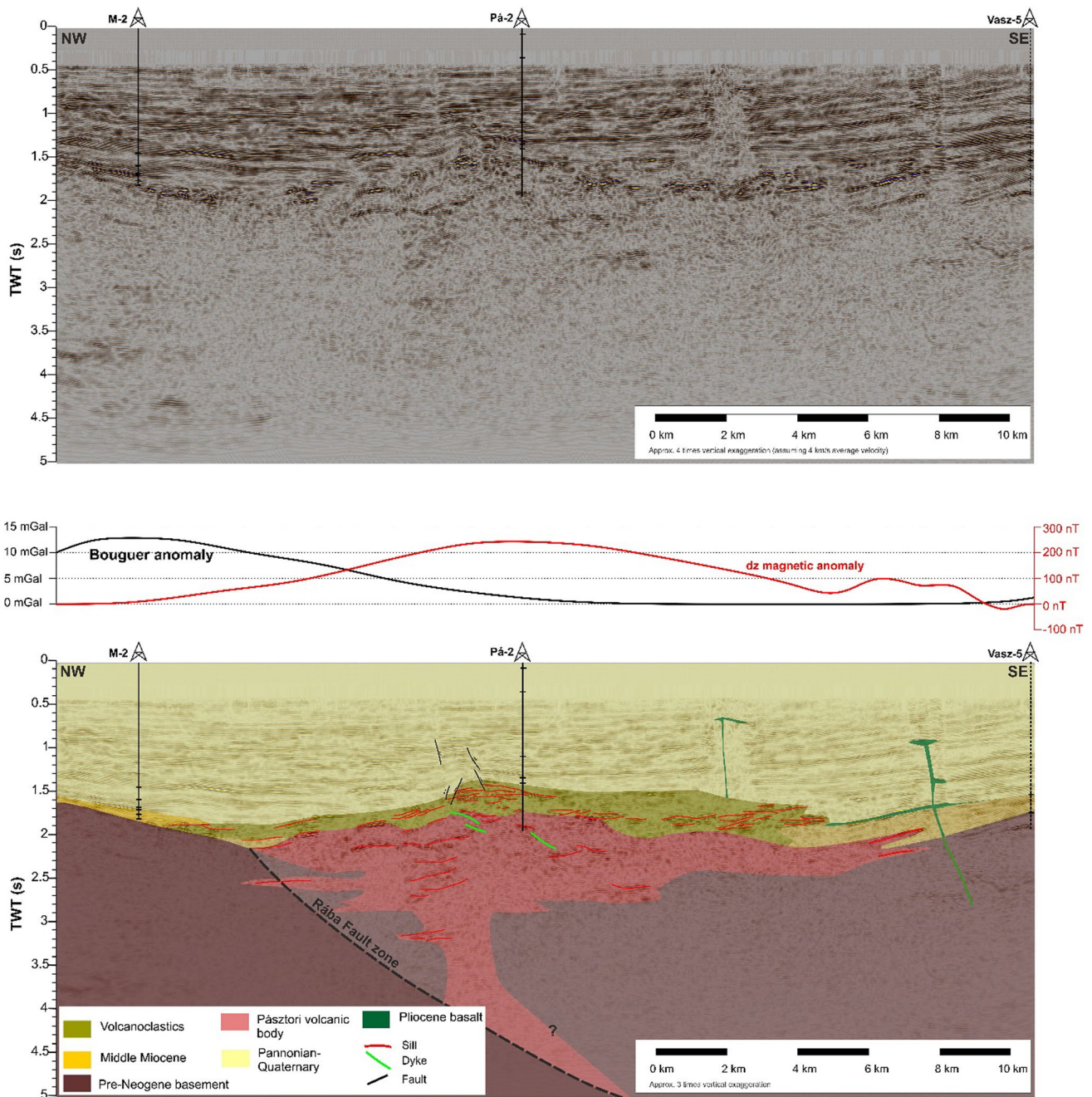


Fig. 2 Interpreted reflection seismic transect calibrated by well data from the southern part of the Danube Basin showing the main (sub-)volcanic bodies and stratigraphy of the Pásztori area. For location, see Fig. 1c. Note that the volcanoclastic succession of the Pásztori volcano is interfingering with the Late Miocene deep lacustrine sediments of Lake Pannon. Location of the Rába fault zone is indicated

based on further seismic and well data (cf., Haas et al. 2010). Note the low Bouguer gravity and high magnetic anomalies above the interpreted volcanic geometry. Basalt bodies are interpreted at multiple levels within the Pannonian (s.l.) succession; further SW-wards basalt volcanoes are located on the surface

units characterized by frequent occurrences of high-amplitude reflectors which are commonly associated with sills or dykes in such volcanic basins (cf., Planke et al. 2005; Spitzer et al. 2005).

Magnetic and gravity anomalies

The distinct, circular magnetic anomaly displayed in Fig. 1c indicates the areal extent of the volcanic rocks. The buried,

Table 2 Densities of crustal units numbered after Haas et al. (2010) used in the gravity modelling

Rock type	Density range (g cm ⁻³)
Gneiss, mica schist (27; Lower Austroalpine Unit)	2.70–2.75
Amphibolite (27; Lower Austroalpine Unit)	2.84–2.85
Phyllite (28; Upper Austroalpine Unit)	2.71–2.77
Limestone, marl (33; Transdanubian Range Unit)	2.54–2.63
Metasiltstone, slate, limestone, metavolcanites (54; Transdanubian Range Unit)	2.54–2.61
Limestone, metavolcanites, dolomite, phyllite (40–54; Transdanubian Range Unit)	2.66–2.71
Phyllite, limestone, sandstone, metavolcanites (42–51; Transdanubian Range Unit)	2.69
Unclassified (88)	2.66–2.75

trachyandesite-trachyte volcano depicted by v pattern covers an area 20 km × 25 km approximately. Figure 1c also shows the spatial distribution of a small-sized basaltic volcanics—buried one green coloured and outcropping one black coloured, respectively.

The studied positive magnetic anomaly shown in Fig. 4a belongs to the significant belt of magnetic anomalies lying on the territory of NW Hungary that coincides with the Rába fault zone (Kiss and Gulyás 2006b) and is related to the tectonically triggered Neogene volcanism on this low-angle-detachment fault system. The overall wavelength of the magnetic anomaly certainly suggests a deeper magnetic source.

In the SE part of the magnetic maps, a group of several sharp, high-intensity positive and negative anomalies occurs produced by small-scale, very shallow sills emplaced within the Pannonian sediments and small-volume basaltic volcanoes (i.e., erosional remnants of maars, tuff rings, scoria cones, lava flows). These signatures reflect erosional remnants, potentially maar diatremes of typical monogenetic volcanic edifices. Such volcanic features were modelled using forward modelling by many authors (e.g., Lindner et al. 2006; Matthes et al. 2010; Blaikie et al. 2014; van den Hove et al. 2015). Magnetic pattern indicates closely spaced magnetic sources with possible remanent magnetization playing a role.

The gravity data were interpolated to the magnetic stations producing a relatively small-sized grid above investigated volcanic structures (42.5 km × 40 km roughly) using a point spacing of 500 m (Fig. 4). The Hungarian HD72/EOV rectangular coordinate system is used, with axes defined as easting (Y) and northing (X). The Bouguer gravity anomalies above the Pásztori volcano are displayed in Fig. 4b. The gravity map reflects the superposed effects of the regional changes in the crystalline pre-Cenozoic basement and crustal structures. The magnitudes of gravity anomalies range from −9.5 mGal¹ to +20 mGal. The positions of boreholes

that are analysed in methodological “Constraints from boreholes” to determine the physical parameters of volcanic rocks are denoted in Fig. 4a, b by black signs with particular names. The modelling by means of the gravity field is more complicated as the Pásztori volcano is not visible in the Bouguer anomaly map. It is due to the small density contrast between the volcanic rocks and the surrounding Miocene sedimentary rocks.

On the Bouguer anomaly map (Fig. 4b), two distinctive reddish gravity highs dominate. The left one of typically elongated shape indicates the presence of elevation in crystalline basement called Mihályi high. The second one in the SE part of the map is caused by the steeply ascending basement under the Bakony Mountains in the Transdanubian Range unit. The significant gravity low shown in Fig. 4b by violet colour indicates the deepening of the sedimentary basin filled by lower density material.

Figure 4 allows to visually compare the calculated magnetic (Fig. 4c) and gravity (Fig. 4d) effects of the resultant 3D model with the observed fields. The main characteristic features on both pairs of the maps are comparable with only little shape differences observable. The corresponding difference maps (Fig. 4a minus Fig. 4c) and (Fig. 4b minus Fig. 4d) displayed in Fig. 5 express the reliability of their fit in the IGMAS+, i.e., the discrepancy between observed and modelled magnetic and gravity values. Globally, the calculated differences are at acceptable low levels, ±25 nT maximally for magnetic maps (Fig. 5a) and +2/−2.5 mGal for gravity ones (Fig. 5b). In the case of magnetic difference map, the erroneous model misfit (very high amplitudes of +600/−400 nT) emerging on the edges of the maar locations (area bounded by a red dashed ellipse in Fig. 5a) is caused by the small number of stations (large station distance of 500 m) by which we can represent the narrow magnetic anomalies due to the shallow small-sized maars. The statistics concerning the comparison of utilized geophysical fields is following: (1) standard deviation (gravity: 0.675 mGal, magnetic: 23.31 nT), (2) variance (gravity:

¹ 1 mGal = 10⁻⁵ m s⁻².

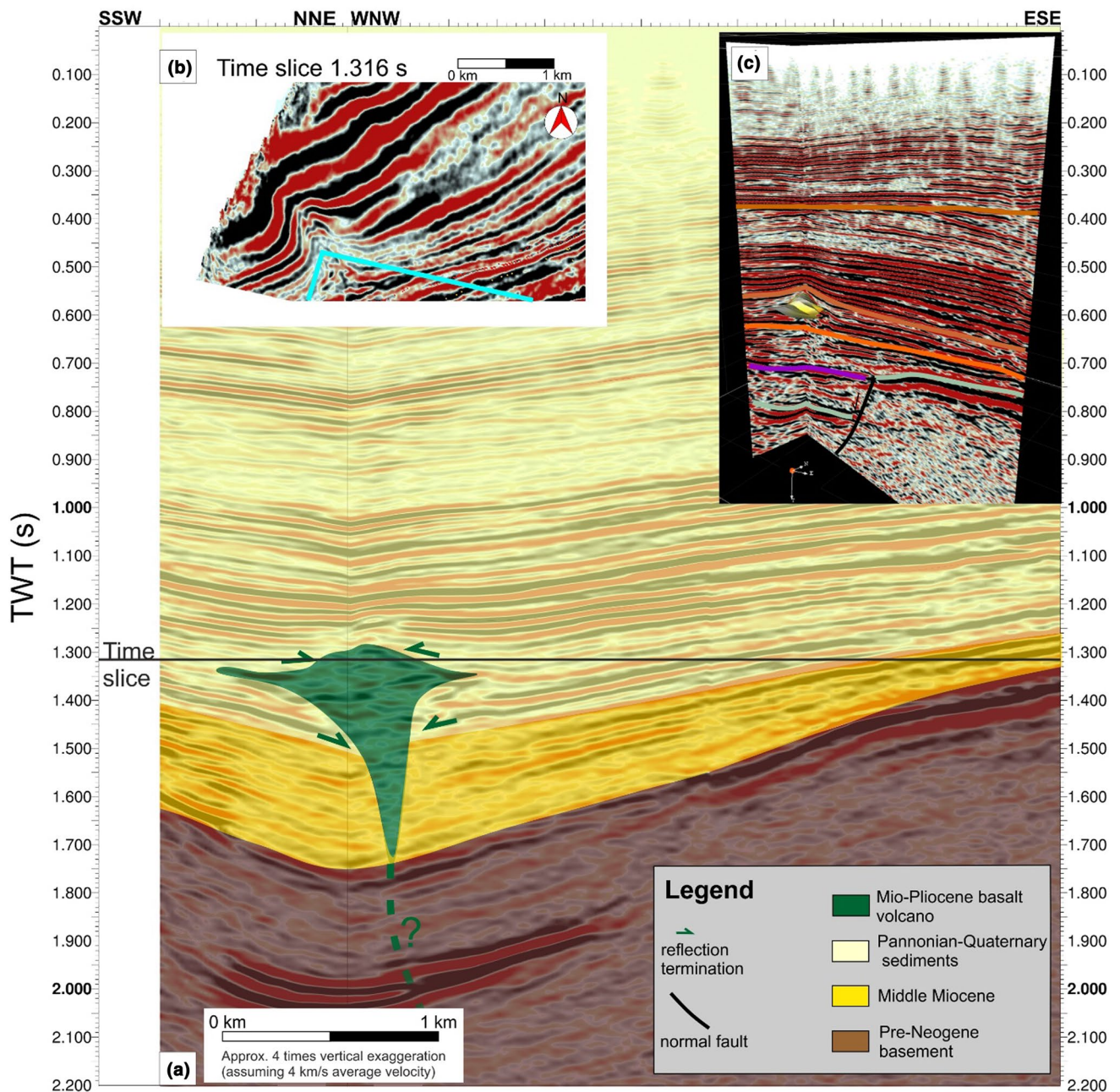


Fig. 3 **a** Interpreted arbitrary line showing a basalt body within Pannonian sediments, **b** seismic time slice showing the chaotic seismic facies of the basalt, **c** 3D image of the arbitrary line and the mapped surface of the basalt body (in yellow). For location, see Fig. 1

0.456 mGal², magnetic: 543.26 nT²), and (3) correlation coefficient (gravity 0.992, magnetic 0.94).

Model of the Pásztori volcano

The final model of the buried Pásztori (trachyandesite-trachyte) volcano consists of three anomalous bodies (see two cross sections in Figs. 6, 3D model in Fig. 7):

- Upper body—~ 0.3–1.8 km-thick layer of volcanoclastics with a top situated at minimal depth of 1.8 km [mean magnetic susceptibility of 0.015 SI based on our measurements of core samples (Table 1) and density of 2.4 g cm⁻³ taken from Eliáš and Uhmán (1968)].
- Middle body—trachyte-to-trachyandesite lava edifice up to 2 km thick with a top situated at minimal depth of 2.3 km. Mean magnetic susceptibility of 0.002 SI and

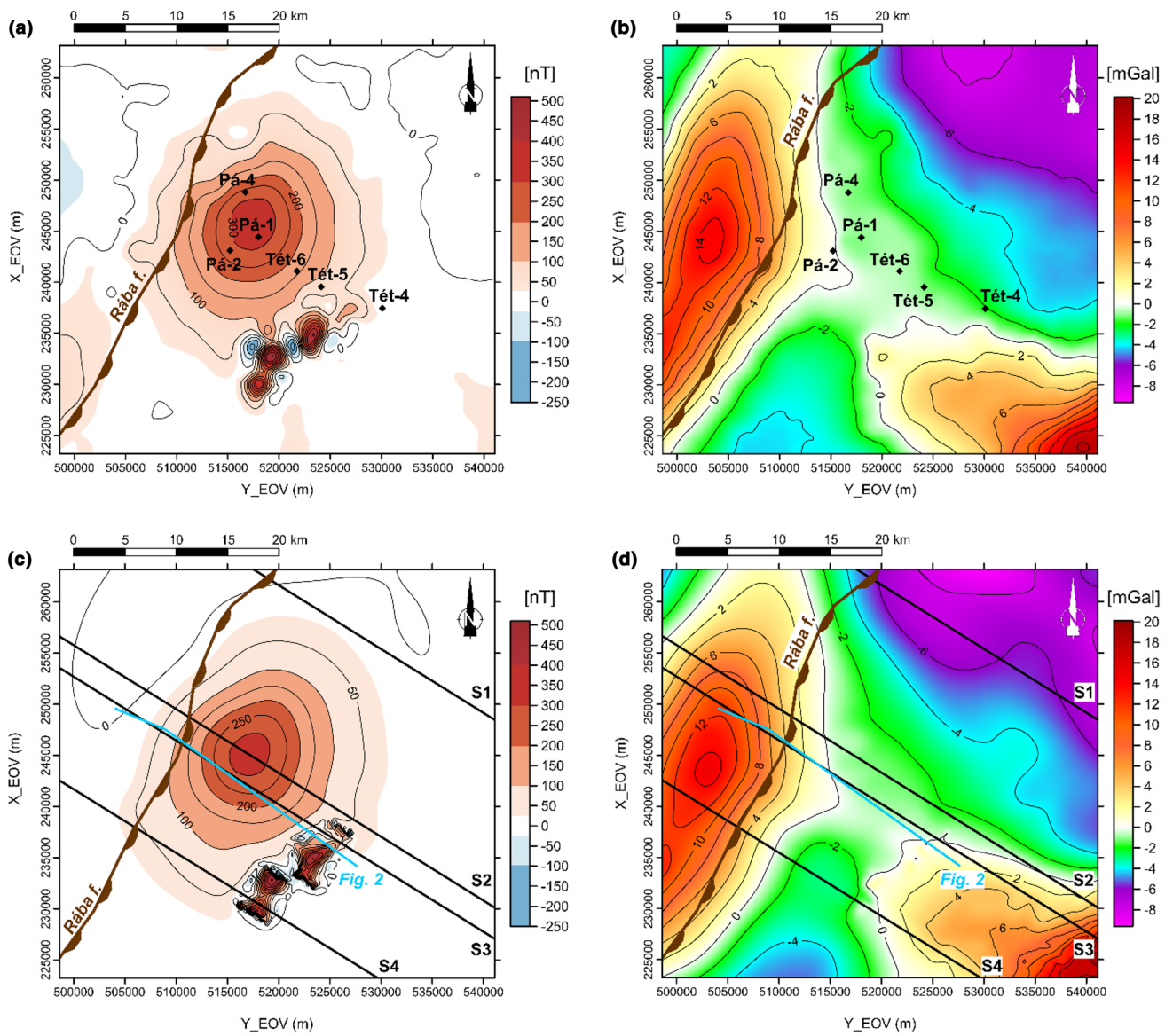
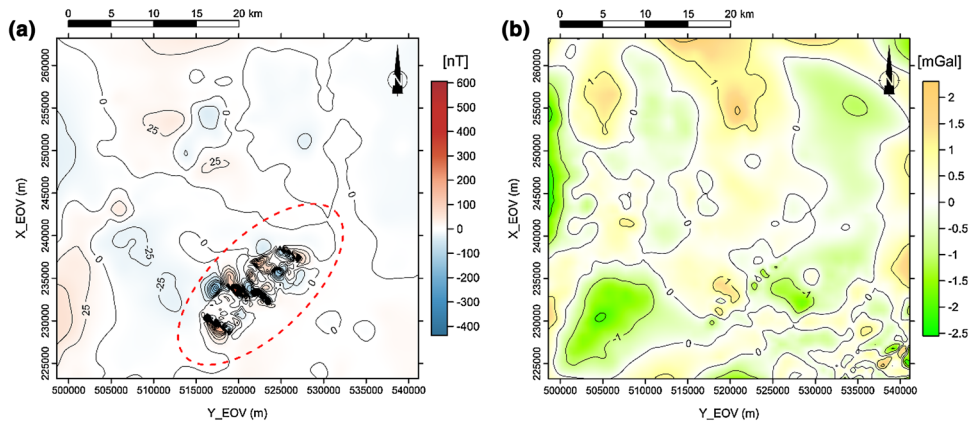


Fig. 4 **a** Magnetic anomaly above the Pásztori volcano, **b** Bouguer gravity anomaly map for a correction density of 2.0 g cm^{-3} , **c** modelled magnetic field, **d** modelled gravity field. Positions of available wells are depicted by black dots with names

Fig. 5 Residual fields: magnetic (**a**) and gravity (**b**)



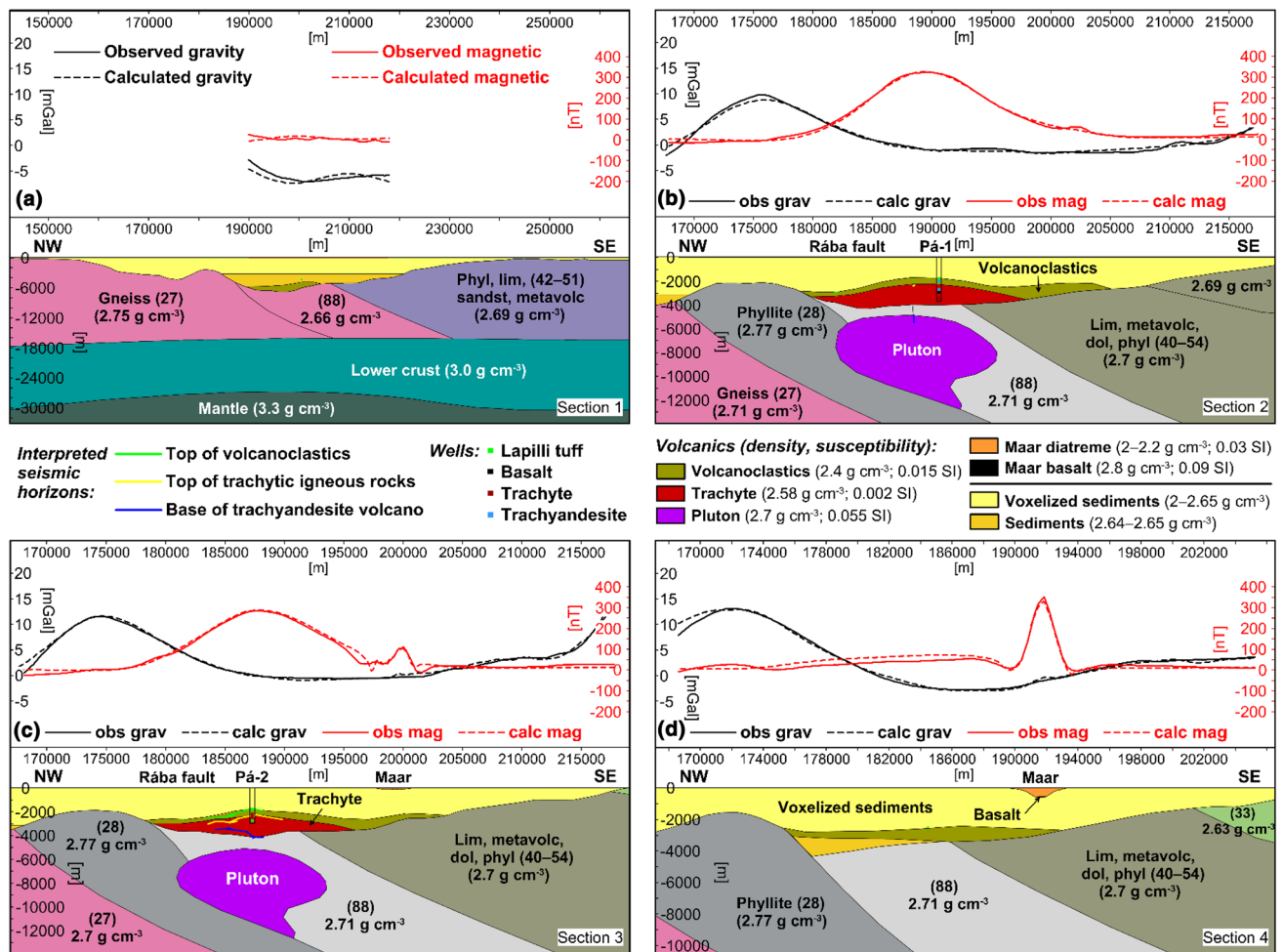


Fig. 6 Four selected cross sections of the final model in Section 1 (a), Section 2 (b), Section 3 (c), and Section 4 (d). Locations of particular sections (S1–S4) oriented in NW–SE direction are drawn by black lines in Fig. 4

density of 2.58 g cm⁻³ are based on our measurements of core samples (Table 1).

- Lower body—assumed deep-seated magma reservoir ~5–15 km depth, estimated susceptibility of 0.055 SI, estimated density of 2.7 g cm⁻³ similar to the surrounding crystalline rocks.

The 3D model is defined from the surface to a 40 km depth. Figure 6 shows reasonable fits between the calculated (dashed line) and observed (solid line) fields. The modelled Pásztori volcano is underlain by an elevated uppermost mantle (Fig. 6a). The density contrast between lower crust and mantle is +0.3 g cm³ (e.g., Lillie et al. 1994; Bielik 1998). The interpreted seismic horizons depicted by three different colours in Fig. 6 constrain the geometry of upper two sheet-like volcanic layers. The volcanic structures are embedded in a layered background, as shown in Fig. 6b, c. The polyhedrons are used in the 3D model to define the bodies, except the light yellow

sediments, where voxelization is applied to allow for the compaction.

The pre-Cenozoic basement exhibits a characteristic morphology, i.e., sub-basins (e.g., Csapod, Kenyeri) are separated by basement highs (e.g., Pinnye, Mihályi). These sub-basins are controlled by major low-angle normal faults of Early-Middle Miocene age (Tari 1996; Szafián et al. 1999). The modelled SE-wards dipping faults system (vertical section 4 in Fig. 6d) is in good agreement with the corresponding part of the regional 2D crustal transect of Szafián et al. (1999). The complexity of the basement in the Bakony Mountains (Transdanubian Range unit) was neglected, only simplified anomalous bodies are used in this part of the model with a constant densities assigned which represent some average densities of a set of present sub-units (for example, body no. 40–54 in the right part of the upper crust in sections portrayed in Sections 2, 3, and 4 of Fig. 6).

The proposed 3D model of Pásztori volcano is also presented in Fig. 7. A 3D representation of the modelled

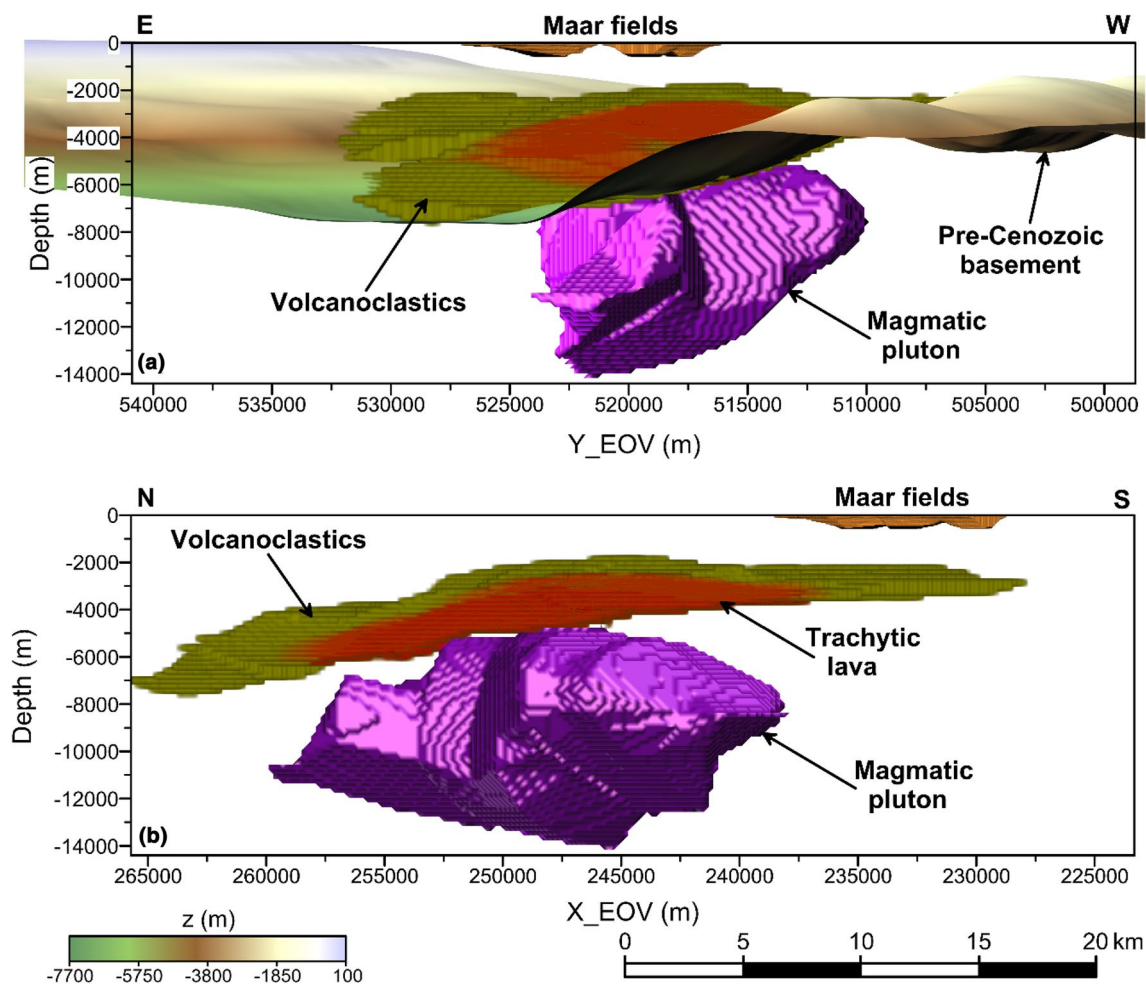


Fig. 7 3D geophysical model of the Pásztori volcano: north view (a) and west view (b)

volcanic bodies by means of voxel cubes is used. Both uppermost volcanic structures (i.e., volcanoclastics and trachytic lava) stretched into the distance in all directions copying the topology of the pre-Cenozoic basement (Fig. 7a). For clarity, we just show the configuration of three volcanic bodies without the pre-Cenozoic basement in Fig. 7b. The top layer of green-yellow volcanoclastics is displayed in a semi-transparent mode allowing the red trachytic lava intrusion below to be visible.

The magnetic susceptibility of the volcanic rocks penetrated by several boreholes (Fig. 4) is not high enough to explain the whole magnetic anomaly. The trachytic lava plays only a very limited role here. It is possible that the rocks penetrated by the wells represent the uppermost level of a larger volcanic–subvolcanic complex (Nemesi et al. 1994). The magmatic pluton (violet coloured in Fig. 6b, c) can be assumed as a reasonable source of the larger part of the distinctive magnetic anomaly.

Model of basalt volcanoes

Basalt volcanism in the Little Hungarian Plain and the nearby Bakony–Balaton Highland Volcanic Field involved large range of eruption styles and associated volcanic forms, from maars through lava lake-filled tuff rings and scoria cones to shield volcanoes (Harangi et al. 1994; Németh and Martin 1999; Németh et al. 2001; Martin and Németh 2004; Németh 2012). Shallow, but broad tuff ring volcanoes in LHPVF have been formed due to the phreatomagmatic explosive eruption caused by mixing between uprising hot basaltic magma and water-saturated clastic sediments in areas where thick Neogene siliciclastic units build-up shallow pre-volcanic strata (Harangi and Harangi 1995; Martin and Németh 2004, 2005). Within the tuff rings, scoria cones and lava lakes were formed when water supply drastically decreased and the eruptions were controlled primarily by the volatile exsolution in the ascending basaltic magma.

Tuff ring and maars are underlain by a diatreme with various depths that are filled by the mobilised host rock and magmatic fragments during the magma–water interaction controlled explosions. Occasionally, such diatremes could contain also coherent basaltic body of the solidified feeder dyke (Lorenz 2003; Haller and Németh 2009; Lefebvre et al. 2016). The tuff rings in this region were subjected to a detailed geophysical survey that revealed significant reservoirs of alginite and basaltic bentonite, minerals utilizable in industry (Tóth 1994).

As the input gravity and magnetic fields do not have a sufficient quality and resolution to model the individual tuff rings or maars, we have created only very simplified schematic model of the basaltic field located on the SE edge of the magnetic ΔZ anomaly (Fig. 4a). The tuff ring/maar model contains two bodies defined on seven vertical sections from the surface up to 800 m depth maximally. Each body consists of two parts with constant physical parameters taken from tables of Tóth (1994):

- Upper cone-shaped diatreme with magnetic susceptibility of 0.03 SI and density of 2.0–2.2 g cm⁻³ (~0–570 m depth, orange colour in Fig. 6c, d).
- Small remnants of basaltic dykes feeder systems up to 250 m thick situated in the lower part of the maars with high magnetic susceptibility of 0.09 SI and density of 2.8 g cm⁻³ (black colour in Fig. 6c, d).

The diatremes are broad with shallowly dipping walls close to the surface, which become more steeply dipping in greater depths (Section 4 in Fig. 6d). The geometries of modelled basalt volcanoes are consistent with the reconstructions of several maar and tuff ring volcanoes from the western Hungarian monogenetic volcanic fields (Németh 2012).

Discussion

The syn- and post-rift evolution of the Pannonian Basin system was associated with extensive volcanic activity. A large amount of volcanological and geochemical case studies analysed the erosional remnants of magmatic rocks on the surface, while understanding the overall tectono-magmatic evolution and the imaging of deeply buried volcanic bodies require a joint geological and geophysical approach (cf., Harangi and Lenkey 2007; Kovács et al. 2012 and references therein). The close link between tectonics and the evolution of volcanic fields has been noted for a long time in connection with sedimentary basins. One of the most spectacular surface examples is the Chaîne des Puys in France, where a series of monogenetic volcanoes are aligned along and evolved in the vicinity of the boundary faults of the

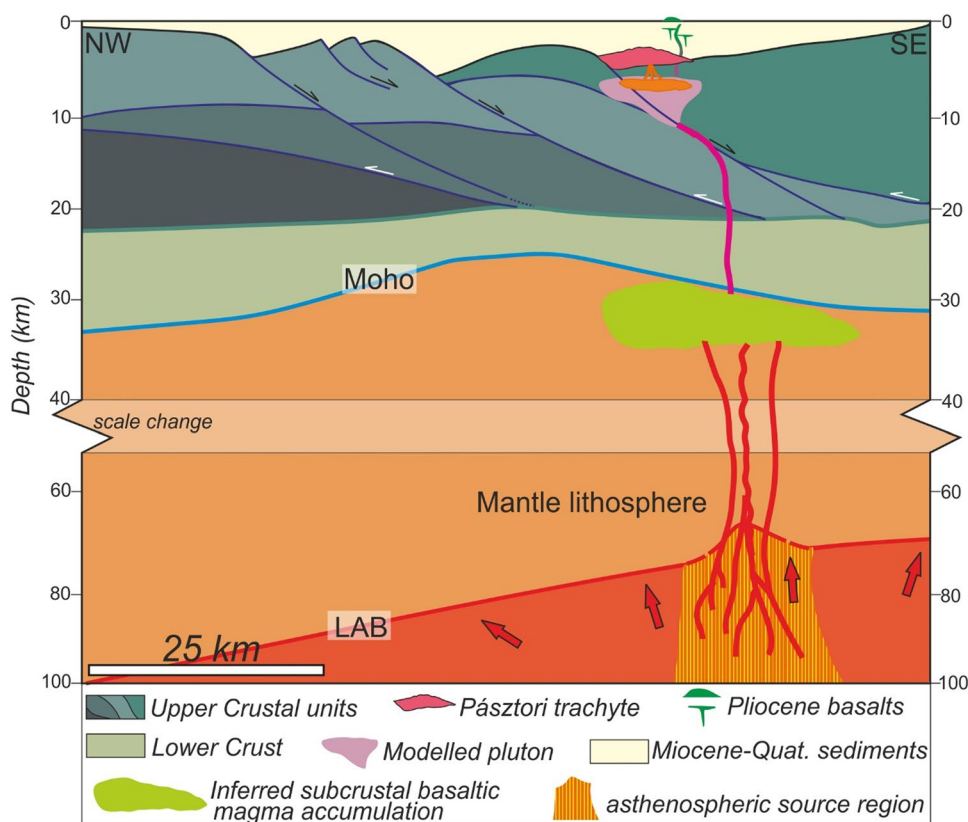
Cenozoic Limagne rift (e.g., Mathieu and Wyk de Vries 2011; Holohan et al. 2013; Petronis et al. 2013; Delcamp et al. 2014), while tectonic control of the volcanism was also pointed out in other areas (Valentine and Perry 2007; Valentine and Hirano 2011; Germa et al. 2013). In this chapter, we discuss our modelling results of the buried Pásztori volcano and its connection to the tectonic evolution of the Danube Basin.

Regional integration

Miocene–Pliocene trachyandesitic and subsequent basaltic volcanism of the Pásztori area is rare, but not unique in the highly extended Pannonian Basin system. A noteworthy feature is that basaltic volcanism culminated after the syn-rift phase of the basin. One of the oldest examples is the Styrian Basin, where ~17.5–14 Ma trachyandesitic volcanism (Harangi et al. 1995b) was followed by alkaline basaltic volcanism between 3.9 and 1.9 Ma (Pécskay et al. 2006). Badenian (~15–14 Ma) potassic trachyandesites were reported from an exploration well near Balatonmária from the Mid-Hungarian Fault Zone (Harangi et al. 1995b; Klébesz et al. 2009). It corresponds with 120 nT (ΔZ) positive magnetic anomaly. In its northern vicinity, basaltic volcanism took place from ~7.9 Ma in the Bakony–Balaton Highland Volcanic Field, creating short wavelength high-amplitude magnetic anomalies. Interestingly, Quaternary (1.6 Ma) potassic trachyandesites were reported from the Apuseni Mountains (Seghedi et al. 2004), where the lithospheric thickness is locally as thick as ~100 km in contrast to the ~50 km in the most extended parts of the basin. In general, alkaline basaltic volcanism occurred during Late Miocene-to-Quaternary times in several sub-basins of the Pannonian region (cf., Harangi et al. 2015). Similar to our modelling results, they are often deeply buried today, for instance below the Danube–Tisza interfluvium in the Kecel Volcanic Field (Fig. 1; Balázs and Nusszer 1987). However, they are well imaged by seismic data (Zelenka et al. 2004) and are associated with significant magnetic anomalies (e.g., Kiss 2013). In the southern part of Slovakia, the Kráľová trachyandesitic volcanic edifice dated as Middle Miocene is located (Sztanó et al. 2016). Analogous to the Pásztori volcano, the Kráľová volcano buried at ~2 km depth is characterized by a distinctive anomalous magnetic pattern and missing signature in the gravity field. Seismic reflection profile data combined with concave/convex features analysis of potential field were used to study the areal shape of the volcano (Hrušecký 1997; Pašteka et al. 2015).

Similar to the above-mentioned examples in our study area in the Danube Basin igneous bodies are imaged, modelled and inferred at different depths (Fig. 8). On the surface, erosional remnants of Latest Miocene–Pliocene (~6–4.5 Ma, Balogh et al. 1986) basaltic volcanism are represented by

Fig. 8 Simplified sketch showing the asthenospheric sourced volcanism in the LHPVF. Note the Pliocene basalt volcanoes on the surface, stalled Pannonian basalt bodies within the Pannonian sedimentary succession, the early Late Miocene Pásztori volcano underlain by the modelled pluton and an inferred massive basaltic magma accumulation below the Moho. Crustal and lithospheric thickness is after Tari et al. (1999), Szafián et al. (1999). LAB lithosphere–asthenosphere boundary. Red arrows indicate inferred mantle convection (cf., Horváth et al. 2015; Balázs et al. 2017)



maars, tuff rings, and scoria cones (e.g., Németh 2012). Small-volume Late Miocene basalt bodies are also interpreted in our seismic data at a depth of ~1000–1750 m within the Pannonian strata. Most probably, they are stuck intrusions creating gentle anticline geometries in the overlying Pannonian siliciclastic sediments (Fig. 3). The earliest Late Miocene Pásztori volcano located in the hanging wall of the Rába detachment is built up by a series of alkaline trachytic lavas and intercalated pyroclastic rocks, overlain by trachyandesitic lava flows and volcanoclastic breccias (Schléder 2001). The extent of the different igneous rocks covers a large area of ca. 350 km² and the height of this paleovolcano from the base could have reached ~1.5 km forming a small island in Lake Pannon. In spite of the large extent of this volcano, it cannot reproduce alone the observed magnetic anomaly of this area. Our geophysical modelling supports the existence of a magmatic pluton below the volcano.

Petrological and geochemical modelling suggested that the trachyandesitic–trachytic evolved magmas could have been developed by fractional crystallization of basaltic magma and they could represent about 20–40% residual part of the parental magma body (Harangi et al. 1995a; Harangi 2001). That could imply a massive mafic cumulative residual body in the crust. The previous gravity modelling and geochemical studies in the similar Nógrád–Gemer Volcanic Field of the Pannonian Basin (e.g., Bielik 2000; Novák et al.

2014) inferred massive magma body below the Moho representing the accumulation of basaltic magma. Furthermore, our potential field modelling yields a magnetic source at a depth of ~5–15 km, suggesting a mid-crustal pluton too (Fig. 7) in agreement with the previous magnetic modelling studies (Kiss 2013). This pluton is located around the upper crustal brittle-ductile transition zone (cf., Lenkey et al. 2002; Balázs et al. 2017), and the magma of the later volcanoes could have ascended in the upper crust along the inherited structures, such as the Rába fault zone.

Tectono-magmatic evolution of the Danube Basin

Extensional deformation in the Pannonian Basin system was diachronous and migrated in time and space between Early and Late Miocene times (for details, see Balázs et al. 2016 and references therein). Recent subsidence history analysis and thermo-mechanical modelling infers an even earlier onset of extension associated with an initial topographic updoming phase controlled by fast asthenospheric uprise from latest Paleogene (Balázs et al. 2017). The hanging wall of the Rába detachment fault in the Danube Basin is overlain by Middle Miocene sediments (Tari and Horváth 2006) implying Middle Miocene peak of extension and associated crustal thinning (Horváth et al. 2015). Then, syn-rift extension gradually ceased between 14 and 8 Ma. After a

short-lived earliest Late Miocene inversion (Horváth 1995), fast subsidence continued in the basin. By that time, the Pannonian lithosphere was already thinned and thermally weakened (Lankreijer 1998), and therefore, it was especially capable for further deformation. The final small normal fault offsets in the Danube Basin (e.g., Fodor et al. 2013), such as along the Rába fault zone, enabled the ascent of the evolved magma from the deeper crustal pluton creating the Pásztori volcano.

It has been shown that passive rifting can initiate further active uprise of the asthenosphere even during the classical “post-rift” phase (Huisman et al. 2001). A series of 2D thermo-mechanical finite-element modelling designed to simulate the back-arc type of lithospheric extension and subsequent post-extensional evolution inferred that asthenospheric asymmetries created during the syn-rift deformation could be significantly attenuated by subsequent convective thermal processes during post-rift times (Balázs et al. 2017). This is associated with uplift and erosion of the basin margins and fast subsidence of the basin centres. This dynamic evolution of the asthenosphere can initiate further asthenospheric sourced basaltic magmatism even a few million years after the prior syn-rift phase.

The main importance of the detachment faults in the Pannonian Basin is that they produce locally extreme lithospheric extension and thus promoting the mantle elevation below and, therefore, producing an optimal place for magma chamber(s). The upwelling basaltic magmas could ascend through the rheologically weakened mantle lithosphere and lower crust and could get stalled in the strong upper crust. Subsequently, they could ascend towards the surface in the vicinity of major shear zones, such as the Rába fault zone creating the Late Miocene–Pliocene basalt volcanoes in the LHP. Such scenarios need to be quantified by further forward modelling.

Conclusions

In this study, we present a new high-resolution 3D geological model of the early Late Miocene Pásztori volcano which is currently buried beneath a 2 km-thick Late Miocene-to-Quaternary sedimentary sequence in the Little Hungarian Plain Volcanic Field in the NW Hungary. The modelling results are coherent with the volcanological inferences concerning the evolution of volcanic systems formed by trachyandesitic and alkaline basaltic magmas. The trachyte is formed by fractional crystallization of basaltic magma in a crustal magma chamber, where the ascending basaltic magma got stuck, because of its high density. Progressive crystallization resulted in low-density residual melt with trachyandesite-to-trachyte composition. Effective segregation of this magma occurred when large

volume of coherent evolved magma was assembled. Eruption of such significant amount of trachyandesite and trachyte magma requires storing of mafic cumulates in the upper crust.

This study illustrates the value of integrated geophysical modelling in the investigation of different types of volcanic features. The resulting model of the Pásztori volcano is based on various geophysical and geological data sets. Two a-priori known geological interfaces, namely pre-Cenozoic basement and Moho depths, were used to define the starting background density model by which the volcanic bodies are surrounded. Moreover, a simplified set of upper crustal units was created that are divided by the main low-angle detachment faults in the surveyed area. Analysis of the volcanic rock samples from several exploration wells allowed to estimate an average value of the densities and induced magnetic susceptibilities of modelled volcano. Seismic data helped to constrain the geometry of the upper two volcanic structures (i.e., volcanoclastics and trachytic–trachyandesitic lava edifice), while the 3D potential field modelling allowed to indicate a deeper crustal magnetic source. The maximal depths achieved for the location of the crustal pluton do not exceed the estimated depths of Curie isotherm in NW Hungary (Kis et al. 1999; Kiss et al. 2005). Presented geophysical model also provides an assessment of subsurface magma volumes, especially valuable in cases when the volcanoes cannot be investigated by surface geological mapping. As a future outlook, it would be interesting to carry out a similar investigation of buried volcanoes on Slovakian part of the Danube Basin to provide an extended insight into the studied topic.

We show that intraplate alkaline volcanism in the Danube Basin commenced at early–Late Miocene times (ca. 11–10 Ma) resulting in a trachyte–trachyandesite volcano at the contemporaneous surface associated with a magmatic pluton located in the upper crust. After a few million years period of quiescence, alkaline basaltic volcanism took place in a close proximity during the classical post-rift phase of the basin. The erosional remnants of this latter phreatomagmatic event are preserved on the surface, while stalled intrusions and the older trachyandesite volcano are mapped on seismic profiles and confirmed by our integrated geophysical modelling. Late Miocene volcanism in the Danube Basin is genetically controlled by ascending asthenosphere related to the Miocene lithospheric extension and the development of the Rába detachment fault zone.

Acknowledgements This work was supported by the Slovak Research and Development Agency under the contracts nos. APVV-16-0146 and APVV-16-0482, partially by the VEGA Slovak Grant Agency under projects nos. 1/0141/15 and 2/0042/15. Contribution from Hungarian National Fund OTKA 109255K is also appreciated, supported through the New National Excellence Program of the Ministry of Human Capacities (Hungary).

References

- Alvers MR, Götze H-J, Barrio-Alvers L, Plonka C, Schmidt S, Lahmeyer B (2014) A novel warped-space concept for interactive 3D-geometry-inversion to improve seismic imaging. *First Break* 32:61–67
- Bada G, Horváth F, Dövényi P, Szafián P, Windhoffer G, Cloetingh S (2007) Present-day stress field and tectonic inversion in the Pannonian basin. *Glob Planet Change* 58:165–180
- Balázs E, Nusszer A (1987) Unterpannonischer Vulkanismus der Beckengebiete Ungarns. *Ann Hung Geol Inst* 69:95–104
- Balázs A, Matenco L, Magyar I, Horváth F, Cloetingh S (2016) The link between tectonics and sedimentation in back-arc basins: new genetic constraints from the analysis of the Pannonian Basin. *Tectonics* 35:1526–1559
- Balázs A, Burov E, Matenco L, Vogt K, Francois T, Cloetingh S (2017) Symmetry during the syn- and post-rift evolution of extensional back-arc basins: The role of inherited orogenic structures. *Earth Planet Sci Lett* 462:86–98
- Balogh K, Árva-Sós E, Pécskay Z, Ravasz-Baranyai L (1986) K/Ar dating of post-Sarmatian alkali basaltic rocks in Hungary. *Acta Mineralogica et Petrographica Szeged* 28:75–93
- Bielik M (1998) Analysis of the gravity field in the Western and Eastern Carpathian junction area: density modeling. *Geol Carpath* 49:75–83
- Bielik M (2000) Regional lithospheric density modelling of the Western Carpathians. In: Atlas of geophysical maps and profiles No. 0801840 301/180. Open file report—Geofond. State Geological Institute of Dionýz Štúr, Bratislava, pp 1–5
- Blaikie TN, Ailleres L, Betts PG, Cas RAF (2014) A geophysical comparison of the diatremes of simple and complex maar volcanoes, Newer Volcanics Province, south-eastern Australia. *J Volcanol Geoth Res* 276:64–81
- Clark DA, Emerson DW (1991) Notes on rock magnetization characteristics in applied geophysical studies. *Expl Geophys* 22:547–555
- Delcamp A, van Wyk de Vries B, Stéphane P, Kervyn M (2014) Endogenous and exogenous growth of the monogenetic Lemp-tégý volcano, Chaîne des Puys, France. *Geosphere* 10:998–1019
- Eliáš M, Uhmam J (1968) Densities of the rocks in Czechoslovakia. Geological Survey, Prague, p 85
- Faccenna C, Becker TW, Auer L, Billi A, Boschi L, Brun JP, Capitanio FA, Funicello F, Horváth F, Jolivet L (2014) Mantle dynamics in the Mediterranean. *Rev Geophys* 52:283–332
- Fodor L, Sztanó O, Magyar I, Törő B, Uhrin A, Várkonyi A, Csillag G, Kövér S, Lantos Z, Tóké L (2013) Late Miocene depositional units and syn-sedimentary deformation in the western Pannonian basin, Hungary. In: Schuster R (ed) 11th workshop on alpine geological studies and 7th European symposium on fossil algae. Abstracts and field guides. *Berichte der Geologischen Bundesanstalt, Schladming*, pp 33–34
- Germa A, Connor LJ, Cañon-Tapia E, Le Corvec N (2013) Tectonic and magmatic controls on the location of post-subduction monogenetic volcanoes in Baja California, Mexico, revealed through spatial analysis of eruptive vents. *Bull Volcanol* 75(12):782
- Götze H-J (2014) Potential method and Geoinformation Systems. In: Freedon W, Nashed MZ, Sonar T (eds) *Handbook of geomathematics*. Springer, Berlin, pp 1–21
- Götze H-J, Lahmeyer B (1988) Application of three-dimensional interactive modelling in gravity and magnetics. *Geophysics* 53:1096–1108
- Götze H-J, El-Kelani R, Schmidt S, Rybakov M, Hassouneh M, Förster H-J, Ebbing J (2007) Integrated 3D density modelling and segmentation of the dead sea transform. *Int J Earth Sci (Geol Rundsch)* 96:289–302
- Gudmundsson MT, Milsom J (1997) Gravity and magnetic studies of the subglacial Grímsvötn volcano, Iceland: Implications for crustal and thermal structure. *J Geophys Res* 102(B4):7691–7704
- Haas J, Budai T, Csontos L, Fodor L, Konrád G (2010) Pre-Cenozoic geological map of Hungary. 1:500000. Geological Institute of Hungary, Budapest
- Haller M, Németh K (2009) Cenozoic diatremes in Chubut, Northern Patagonia, Argentina. In: 3ICM international maar conference, Malargüe, Argentina, extended abstract, p 23
- Harangi S (2001) Neogene magmatism in the Alpine-Pannonian Transition Zone—a model for melt generation in a complex geodynamic setting. *Acta Vulcanol* 13:25–39
- Harangi R, Harangi S (1995) Volcanological study on the Neogene basaltic volcano of Sághegy (Little Hungarian Plain Volcanic Field, Western Hungary). In: Downes H, Vaselli O (eds) *Neogene and related volcanism in the Carpatho–Pannonian Region*. *Acta Vulcanology*, vol 7, pp 189–197
- Harangi S, Lenkey L (2007) Genesis of the Neogene to Quaternary volcanism in the Carpathian–Pannonian region: role of subduction, extension, and mantle plume. *Geol Soc Am Spec Pap* 418:67–92
- Harangi S, Vaselli O, Kovács R, Coradossi N, Tonarini S, Ferraro D (1994) Volcanological and magmatological studies on the Neogene basaltic volcanoes of the Southern Little Hungarian Plain, Western Hungary. *Min Petr Acta* 37:183–197
- Harangi S, Vaselli O, Tonarini S, Szabó C, Harangi R, Coradossi N (1995a) Petrogenesis of Neogene extension-related alkaline volcanic rocks of the Little Hungarian Plain Volcanic Field (Western Hungary). *Acta Vulcanol* 7:173–187
- Harangi S, Wilson M, Tonarini S (1995b) Petrogenesis of Neogene potassic volcanic rocks in the Pannonian Basin. *Acta Vulcanol* 7:125–134
- Harangi S, Jankovics ME, Sági T, Kiss B, Lukács R, Soós I (2015) Origin and geodynamic relationships of the Late Miocene to Quaternary alkaline basalt volcanism in the Pannonian Basin, eastern-central Europe. *Int J Earth Sci (Geol Rundsch)* 104:2007–2032
- Hetényi G, Ren Y, Dando B, Stuart GW, Hegedűs E, Kovács AC, Houseman GA (2015) Crustal structure of the Pannonian Basin: the AlCaPa and Tisza Terrains and the Mid-Hungarian Zone. *Tectonophysics* 646:106–116
- Holohan EPR, Walter T, Schöpfer MPJ, Walsh JJ, Van Wyk De Vries B, Troll R (2013) Origins of oblique-slip faulting during caldera subsidence. *J Geophys Res Solid Earth* 118:1778–1794
- Horváth F (1995) Phases of compression during the evolution of the Pannonian Basin and its bearing on hydrocarbon exploration. *Mar Pet Geol* 12(8):837–844
- Horváth F, Musitz B, Balázs A, Végh A, Uhrin A, Nádor A, Koroknai B, Pap N, Tóth T, Wórum G (2015) Evolution of the Pannonian basin and its geothermal resources. *Geothermics* 53:328–352
- Hruščeký I (1997) Central part of the Danube basin in Slovakia—geophysical-geological model and its influence to the oil/gas potential of the region. Ph.D. thesis, Faculty of Natural Sciences, Comenius University, Bratislava, p 112 (in Slovak)
- Huismans RS, Podladchikov YY, Cloetingh S (2001) Dynamic modelling of the transition from passive to active rifting: application to the Pannonian basin. *Tectonics* 20:1021–1039
- Hunt CP, Moskowitz BP (1995) Magnetic properties of rocks and minerals. In: Ahrens TJ (ed) *Rock physics and phase relations: a handbook of physical constants*, vol 3. American Geophysical Union, Washington, DC, pp 189–204
- Kis KI, Agocs WB, Meyerhoff AA (1999) Magnetic sources from vertical magnetic anomalies. *Geophys Trans* 42(3–4):133–157
- Kiss J (2006) Bouguer anomaly maps of Hungary. *Geophys Trans* 45:99–104
- Kiss J (2009) A CEL08 szélveny geofizikai vizsgálata. *Magy Geofiz* 50(2):59–74 (Hungarian)

- Kiss J (2013) Magyarországi geomágnese adatok és feldolgozások: spektrálanalízis és térképi feldolgozások. *Magyar Geofizika* 54(2):89–114 (**Hungarian**)
- Kiss J, Gulyás Á (2006a) Gravity Bouguer anomaly map of Hungary, 1:500000. Eötvös Loránd Geophysical Institute of Hungary, Budapest
- Kiss J, Gulyás Á (2006b) Magnetic ΔZ anomaly map of Hungary, 1:500000. Eötvös Loránd Geophysical Institute of Hungary, Budapest
- Kiss J, Szarka L, Prácser E (2005) Second-order magnetic phase transition in the Earth. *Geophys Res Lett* 32:L24310
- Klébesz R, Harangi S, Ntafos T (2009) Petrogenesis of the ultrapotassic trachyandesite at Balatonmária. *Földtani Kozlony* 139(3):237–250 (**Hungarian**)
- Konecný V, Kovác M, Lexa J, Šefara J (2002) Neogene evolution of the Carpatho–Pannonian region: an interplay of subduction and back-arc diapiric uprise in the mantle. *EGU Stephan Mueller Spec Publ Ser* 1:105–123
- Kőrösy L (1987) Hydrocarbon geology of the Little Plain in Hungary. *Általános Földtani Szemle* 22:99–174 (**Hungarian with English summary**)
- Kovács I, Falus G, Stuart G, Hidas K, Szabó C, Flower MFJ, Hegedűs E, Posgay K, Zilahi-Sebess L (2012) Seismic anisotropy and deformation patterns in upper mantle xenoliths from the central Carpathian–Pannonian region: asthenospheric flow as a driving force for Cenozoic extension and extrusion? *Tectonophysics* 514–517:168–179
- Kronome B, Baráth I, Nagy A, Uhrin A, Maros D, Berka R, Černák R (2014) Geological model of the Danube Basin: transboundary correlation of geological and geophysical data. *Slov Geol Mag* 14(2):17–35
- Lankreijer A (1998) Rheology and basement control on extensional basin evolution in Central and Eastern Europe: variscan and Alpine Carpathian–Pannonian tectonics. *Vrije Universiteit, Faculty of Earth Sciences, Amsterdam*, p 158
- Lefebvre NS, White JDL, Kjarsgaard BA (2016) Arrested diatreme development: Standing Rocks East, Hopi Buttes, Navajo Nation, USA. *J Volcanol Geotherm Res* 310:186–208
- Lenkey L, Dóvényi P, Horváth F, Cloetingh SAPL. (2002) Geothermics of the Pannonian basin and its bearing on the neotectonics. In: Cloetingh SAPL, Horváth F, Bada G, Lankreier AC (eds) *Neotectonics and surface processes: the Pannonian Basin and Alpine/Carpathian System*. *EGU Stephan Mueller Special Publication Series* 3, pp 29–40
- Lillie R, Bielik M, Babuška V, Plomerová J (1994) Gravity modeling of the lithosphere in the Eastern Alpine–Western Carpathian–Pannonian region. *Tectonophysics* 231(4):215–235
- Lindner H, Gabriel G, Götte H-J, Kaeppler R, Suhr P (2006) Geophysical and geological investigation of maar structures in the Upper Lusatia region (East Saxony). *Z dt Ges Geowiss* 157(3):355–372
- Lorenz V (2003) Maar-diatreme volcanoes, their formation, and their setting in hard-rock or soft-rock environments. *GeoLines* 15:72–83
- Maros D, Maigut V (eds) (2011) Pre-Cenozoic model horizon grid for Supra-Regional Area. In: *Enclosure 1.15*. 1:500000. Towards sustainable cross-border geothermal energy utilization. *Transenergy—transboundary geothermal energy resources of Slovenia, Austria*
- Martin U, Németh K (2004) Mio/Pliocene phreatomagmatic volcanism in the Little Hungarian Plain Volcanic Field (Hungary) and the western margin of the Pannonian Basin (Austria, Slovenia). In: Budai T (ed) *Mio/Pliocene phreatomagmatic volcanism in the western Pannonian Basin*. *Geologica Hungarica Series Geologica*, Geological Institute of Hungary, Budapest, pp 153–184
- Martin U, Németh K (2005) Eruptive and depositional history of a Pliocene tuff ring that developed in a fluvio-lacustrine basin: Kissomlyó volcano (western Hungary). *J Volcanol Geotherm Res* 147(3–4):342–356
- Martin U, Németh K (2007) Blocky versus fluidal peperite textures developed in volcanic conduits, vents and crater lakes of phreatomagmatic volcanoes in Mio/Pliocene volcanic fields of Western Hungary. *J Volcanol Geotherm Res* 159(1):164–178
- Matenco L, Radivojević D (2012) On the formation and evolution of the Pannonian Basin: Constraints derived from the structure of the junction area between the Carpathians and Dinarides. *Tectonics* 31(6):TC6007
- Mathieu L, Van Wyk de Vries B (2011) The impact of strike-slip, transtensional and transpressional fault zones on volcanoes. Part 1: Scaled experiments. *J Struct Geol* 33(5):907–917
- Matthes H, Kroner C, Jahr T, Kämpf H (2010) Geophysical modelling of the Ebersbrunn diatreme, western Saxony, Germany. *Near Surf Geophys* 8(4):311–319
- Mattick RE, Teleki PG, Phillips RL, Clayton JL, Dávid G, Pogácsás G, Bardócz B, Simon E (1996) Structure, stratigraphy and petroleum geology of the Little Plain Basin, Northwestern Hungary. *AAPG Bull* 80:1780–1800
- McLean CE, Brown DJ, Rawcliffe HJ (2016) Extensive soft-sediment deformation and peperite formation at the base of a rhyolite lava: Owyhee Mountains, SW Idaho, USA. *Bull Volcanol* 78(6):42
- Mészáros F, Zilahi-Sebes L (2001) Compaction of sediments with great thickness in the Pannonian Basin. *Geophys Trans* 44:21–48
- Nemesi L, Hobot J, Kovácsvölgyi S, Milánkovich A, Pápa A, Stomfai R, Varga G (1994) A kistárolás medence aljzatának és kéregszekretének kutatása az ELGI-ben 1982–90 között. *Geophys Trans* 39:193–223 (**Hungarian**)
- Németh K (2012) An overview of the monogenetic volcanic fields of the Western Pannonian Basin: Their field characteristics and outlook for future research from a global perspective. In: Stoppa F (ed) *Updates in volcanology—a comprehensive approach to volcanological problems*. InTech Europe, Rijeka, pp 27–52
- Németh K, Martin U (1999) Late Miocene paleo-geomorphology of the Bakony–Balaton Highland volcanic field (Hungary) using physical volcanology data. *Z Geomorphol* 43(4):417–438
- Németh K, Martin U, Harangi Sz (2001) Miocene phreatomagmatic volcanism at Tihany (Pannonian Basin, Hungary). *J Volcanol Geotherm Res* 111(1–4):111–135
- Németh K, Pécskay Z, Martin U, Gmélíng K, Molnár F, Cronin SJ (2008) Hyaloclastites, peperites and soft-sediment deformation textures of a shallow subaqueous Miocene rhyolitic dome-cryptodome complex, Pálháza, Hungary. *Geol Soc Lond Spec Publ* 302:63–86
- Novák A, Klébesz R, Szabó C, Wesztergom V, Patkó L, Liptai N, Ádam A, Semenov VY, Lemperger I, Kis A, Gribovszki K (2014) Combined geophysical (magnetotellurics) and geochemical results for determination of the Lithosphere–Asthenosphere Boundary (LAB) beneath the Nógrád–Gömör volcanic field. 22nd EM induction workshop, Weimar, Germany, p 4
- Pašteka R, Hronček S, Ihring P, Božanský M, Putiška R (2015) Concave and convex features analysis of Bouguer gravity field with following qualitative interpretation. 77th EAGE conference and exhibition, IFEMA, Madrid, Spain, extended abstract, p 5
- Pécskay Z, Lexa J, Szakács A, Seghedi I, Balogh K, Konecný V, Zelenka T, Kovacs M, Póka T, Fülöp A, Márton E, Panaiotu C, Cvetković V (2006) Geochronology of Neogene magmatism in the Carpathian arc and intra-Carpathian area. *Geol Carpath* 57(6):511–530
- Petronis MS, Delcamp A, Van Wyk De Vries B (2013) Magma emplacement into the Lemptégy scoria cone (Chaîne Des Puys, France) explored with structural, anisotropy of magnetic susceptibility, and paleomagnetic data. *Bull Volcanol* 75:753
- Planke S, Rasmussen T, Rey SS, Myklebust R (2005) Seismic characteristics and distribution of volcanic intrusions and hydrothermal

- vent complexes in the Vøring and Mørebasins. In: Dore AG, Vining BA (eds) *Petroleum geology: North-West Europe and global perspectives—Proceedings of the 6th petroleum geology conference*, vol 6. Petroleum Geology Conferences Ltd., London, Geological Society, pp 833–844
- Reynisson RF, Ebbing J, Skilbrei JR (2009) The use of potential field data in revealing the basement structure in sub-basaltic settings: an example from the Møre margin, offshore Norway. *Geophys Prospect* 57:753–771
- Rollet N, Déverchère J, Beslier MO, Guennoc P, Réhault JP, Sosson M, Truffert C (2002) Back-arc extension, tectonic inheritance, and volcanism in the Ligurian Sea, western Mediterranean. *Tectonics* 21(3): 6–16–23
- Schléder Z (2001) Pásztori koryéki fúrasok miocén vulkáni közettani és geokémiai vizsgálata. M.Sc. thesis, Eötvös Loránd University, Budapest (**in Hungarian**)
- Schmid SM, Bernoulli D, Fügenschuh B, Matenco L, Schefer S, Schuster R, Tischler M, Ustaszewski K (2008) The Alpine–Carpathian–Dinaridic orogenic system: correlation and evolution of tectonic units. *Swiss J Geosci* 101:139–183
- Schmidt S, Plonka C, Götze H-J, Lahmeyer B (2011) Hybrid modelling of gravity, gravity gradients and magnetic fields. *Geophys Prospect* 59(6):1046–1051
- Schmidt S, Barrio-Alvers L, Götze H-J (2015) IGMAS+: Interactive Geophysical Modelling ASistant. Software tutorial, <http://www.potentialgs.com>, p. 59
- Seghedi I, Downes H, Szakács A, Mason PRD, Thirlwall MF, Roşu E, Pácskay Z, Márton E, Panaiotu C (2004) Neogene–Quaternary magmatism and geodynamics in the Carpathian–Pannonian region: a synthesis. *Lithos* 72:117–146
- Spitzer R, White RS, Team iSimm (2005) Advances in seismic imaging through basalts: a case study from the Faroe–Shetland Basin. *Pet Geosci* 11:147–156
- Szabó Z, Páncsics Z (1999) Rock densities in the Pannonia basin—Hungary. *Geophys Trans* 42:5–27
- Szafián P, Tari G, Horváth F, Cloetingh S (1999) Crustal structure of the Alpine–Pannonian transition zone: a combined seismic and gravity study. *Int J Earth Sci (Geol Rundsch)* 88:98–110
- Sztanó O, Kováč M, Magyar I, Šujan M, Fodor L, Uhrin A, Rybár S, Csillag G, Tőkés L (2016) Late Miocene sedimentary record of the Danube/Kisalföld Basin: interregional correlation of depositional systems, stratigraphy and structural evolution. *Geol Carpath* 67:525–542
- Tari G (1996) Neotectonics of the Danube Basin (NW Pannonian Basin, Hungary). In: Ziegler PA, Horváth F (eds) *Peri-Tethys memoir 2: structure and prospects of alpine basins and forelands*, vol 2. *Mém Mus natn Hist nat*, Paris, pp 439–454
- Tari G, Horváth F (2006) Alpine evolution and hydrocarbon geology of the Pannonian Basin: an overview. In: Golonka J, Picha FJ (eds), *The Carpathians and their foreland: Geology and hydrocarbon resources*. AAPG Memoir 84, Chap. 19, 605–618
- Tari G, Dovenyi P, Dunkl I, Horvath F, Lenkey L, Stefanescu M, Szaifán P, Toth T (1999) Lithospheric structure of the Pannonian basin derived from seismic, gravity and geothermal data. In: Durand B, Jolivet L, Horvath F, Serrane M (eds), *The Mediterranean basins: extension within the Alpine Orogen*, vol 156. Geological Society (London) Special Publication, London, pp 215–250
- Tóth C (1994) Geophysical investigation of tuff rings in the Keme-neshát. *Geophys Trans* 39:161–191 (Hungarian)
- Tschirhart V, Pehrsson SJ (2016) New insights from geophysical data on the regional structure and geometry of the southwest Thelon Basin and its basement, Northwest Territories, Canada. *Geophysics* 81(5):B167–B178
- Valentine GA, Hirano N (2010) Mechanisms of low-flux intraplate volcanic fields—basin and range (North America) and northwest Pacific Ocean. *Geology* 38(1):55–58
- Valentine GA, Perry FV (2007) Tectonically controlled, time-predictable basaltic volcanism from a lithospheric mantle source (central Basin and Range Province, USA). *Earth Planet Sci Lett* 261(1):201–216
- van den Hove JC, Ailleres L, Betts PG, Cas RAF (2015) Subsurface structure of a large basaltic maar volcano examined using geologically constrained potential field modelling, Lake Purrumbete Maar, Newer Volcanics Province, southeastern Australia. *J Volcanol Geotherm Res* 304:142–159
- Wamalwa AM, Mickus KL, Serpa LF (2013) Geophysical characterization of the Menengai volcano, Central Kenya Rift from the analysis of magnetotelluric and gravity data. *Case Hist Geophys* 78(4):B187–B199
- Wijbrans J, Németh K, Martin U, Balogh K (2007) ⁴⁰Ar/³⁹Ar geochronology of Neogene phreatomagmatic volcanism in the western Pannonian basin, Hungary. *J Volcanol Geotherm Res* 164:193–204
- Zelenka T, Balázs E, Balogh K, Kiss J, Kozák M, Nemesi L, Pécskay Z, Püspöki Z, Cs R, Széky-Fux V, Újfalussy A (2004) Buried Neogene volcanic structures in Hungary. *Acta Geol Hung* 47(2–3):177–219